

## Flame Shape Prediction with Artificial Neural Network

Sameer Dubey<sup>A\*</sup> and Anil Dubey<sup>B</sup>

<sup>A</sup> Mechanical Engineering Department, Osmania University, Hyderabad, India

<sup>B</sup> Mechanical Engineering Department, Biju Patnaik University of Technology, Rourkela, India

Accepted 10 January 2014, Available online 01 February 2014, **Special Issue-2, (February 2014)**

### Abstract

A flame shape descriptor based on coordinates of edge of a flame is proposed. Artificial Neural Network is used to predict flame image edges. A flame with constant x-coordinate is used in the present study. Y-coordinates of flame edge are predicted using neural network. Recognition experiments were carried out using flame image sampled from a burning candle. The results show a good recognition effectiveness of 89.206 for predicting the next image in the sequence. This work finds its use in all industries which use flames controlled by human observation e.g. rotary kiln, sponge iron recycler pots, flame flaring arrangements in refineries etc.

**Keywords:** Artificial Neural Network, Flame shapes Prediction, Automation, Flame shape prediction, Automatic Flame Control.

### 1. Introduction

Flame shape is an important observed characteristic of flames. It can be used to scale flame properties such as heat release rates and radiation. Flame shape is affected by fuel type, oxygen levels in the oxidizer, inverse burning and gravity. The object of this study is to develop an algorithm that learns behavior of flame in a particular environment. The sample data is used to predict flame shape in next instant. Flame edge coordinates are generated using edge detection. This profile coordinate is given as training to the back propagation neural network. The algorithm generates flame coordinate in next instant with appreciable degree of accuracy. This helps in predicting shape of flame in the next instant.

Many studies have been conducted to predict the shape of flame. Each had its own limitations. Studies conducted in microgravity in Apollo mission (S.S. Krishnan et al, 2008) used a spherical coordinate equation to model flame shape. They studied the flame lengths and widths predicted by various models including the Roper model. They concluded that these models were able to predict the lengths of experimental buoyant and non-buoyant laminar normal diffusion flames (NDFs) accurately but noted that very few models could be used to predict flame widths accurately. The Roper flame shape model was extended to predict complete flame shapes of laminar gas jet normal and inverse diffusion flames on round burners. The Spalding model was extended to inverse diffusion flames. The model was unable to predict the back diffusion close to the burner. Obscuration of the flame by soot prevented an exact comparison in the higher oxygen flames. The

model cannot account for changes in flame shape arising from change in gravity level. A combined analytical and experimental study (Sunderland et al, 2010) was performed to determine the length and width of a candle flame. Measurements were made of laminar steady flames from photographs of straight-wick candles. The wicks studied ranged in diameter from about 1 to 9 mm, and in height from about 2 to 10 mm, with aspect ratios (diameter to length) of 0.1 to 2. With slight adjustment to a constant, the width of the flame was well predicted, and the prediction for the flame height was about 60% too high and offset.

Flame-sheet shapes (Xu F et al, 2000) were measured from photographs using a CH optical filter to distinguish flame-sheet boundaries in the presence of blue CO<sub>2</sub> and OH emissions and yellow continuum radiation from soot. Flame-shape predictions were based on simplified analyses using the boundary layer approximations along with empirical parameters to distinguish flame-sheet and luminous-flame (at the laminar smoke point) boundaries. Finally, luminous flame lengths at laminar smoke-point conditions were roughly twice as long as flame-sheet lengths at comparable conditions.

A flame was studied by adding vortex flows (Keng Hoo Chuah et al, 2007) around Burke-Schumann diffusion flames to predict the flame heights and the flame shapes of small fire whirls. The same is validated experimentally. For purpose of comparison visible flames from the video camera were taken.

(F. C. Christo et al, 1996) used an Integrated PDF/Neural Network approach for simulation of turbulent flames. When difficulties of neural network convergence arise then a histogram redistribution approach is used to smooth the PDF's. (Zang Hong-Liang et al, 2008) employs

\*Corresponding author: Sameer Dubey

Author/Reference	Burke-Schumann	Roper	Spalding	Chung and Law
Axial Diffusion	Neglected	Neglected	Neglected	Included
Axial Convection	Included	Included	Included	Included
Radial Diffusion	Included	Included	Included	Included
Radial Convection	Neglected	Included	Included	Neglected
Buoyancy Effects	Neglected	Included	Neglected	Neglected
Infinite Domain	Neglected	Included	Included	Neglected
Co-Flow	Included	Neglected	Neglected	Included

the flame shape descriptor as the input to neural network. The flame image recognition was studied by the methods of the artificial neural network (ANN) and the Support Vector Machine (SVM) respectively. The highest recognition rate was 88.83% for SVM and 87.38% for ANN. This neural network based flame controller regulates fuel valve by determining centroid of flame. This neural network is not robust enough to predict the flame edges. In (Mark G. Allen et. al., 1993) a combustion system for automatic, real-time control of a combustion process is described. This can be applied with significant advantage to a Wide range of furnaces, boilers and combustion processes. But Flame shape adjustment is achieved by using an optical sensor. In (Hamid A. Abbasi et .al. 2004) flame profile detection by means of detecting heat transfer profiles is used. This method of control is erroneous because of inaccurate edges detected by heat profiles.

A comparison of other numerical methods used to ascertain flame profiles which fail to consider all the determinants is presented in a tabular format.

Hence a robust flame shape prediction algorithm is required. This would enable us to automate industrial process which requires manual "watching flame" operation to control combustion process or to help a robot navigate through fire obstacles.

### 2. Flame Shape

A Flame indicates combustion status in some cases while in others it tells whether flame is under control or not. According to the operation of "Watching Flame" a flame's starting position  $P_0$ ; its deflection from major axis and its maximum height  $P_{max}$  are important parameters. Judging these parameters tell an operator about the condition of flame.

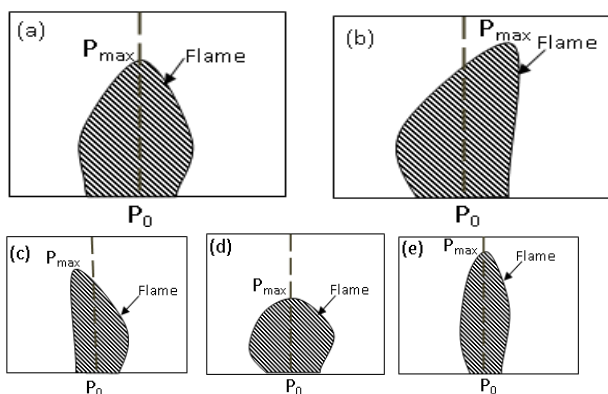


**Fig.1:** Sketches For Observed Flame shapes(a)Normal Flame shape (b) Right Deflected Flame(c) Left Deflected Flame (d) Fat and Short Flame (e) Thin and Long Flame

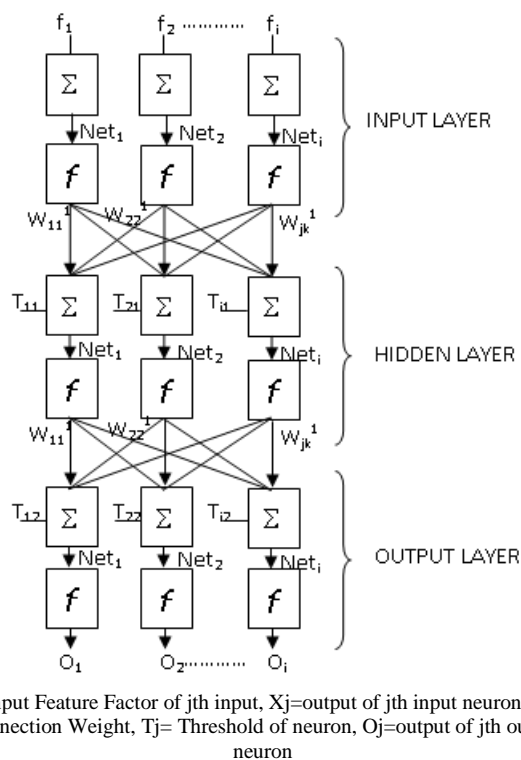
### 3. Flame Shape Descriptors

Y-coordinate of a flame's edge on an image is taken as flame shape descriptor. Flame is assumed to be constant in

X-axis in this study. In Image Processing a flame image's edge is found by deciding a certain intensity level of the image at which the logical flame edge is assumed to exist. Shape contour exists as a set of pixel  $\{x(i), y(i), i=1, 2, 3...N-1\}$ , where N is Number of contour edge point. Since different flame images have different contour pixel. A normalized shape contour must be used. The normalized shape contour has 84 edge points.

### 4. Recognition Methods

Artificial Neural Networks are inspired from the biological world. Different neural network algorithms were tried for the case presented. Finally a classic feed forward back propagation neural network is employed for flame image recognition. Its detailed structure is shown in Fig.



$F_j$ =Input Feature Factor of  $j$ th input,  $X_j$ =output of  $j$ th input neuron,  $W_j$ = Connection Weight,  $T_j$ = Threshold of neuron,  $O_j$ =output of  $j$ th output neuron

**Fig 2:** Feed forward Back Propagation Neural Network

Each neuron receives a signal from the neurons in the previous layer, and each of those signals is multiplied by a separate weight value. The weighted inputs are summed, and passed through a limiting function which scales the

output to a fixed range of values. The output of the limiter is then broadcast to all of the neurons in the next layer. So, to use the network to solve a problem, we apply the input values to the inputs of the first layer, allow the signals to propagate through the network, and read the output values.

A Levenberg-Marquardt algorithm is used for non-linear optimization. Like the quasi-Newton methods, the Levenberg-Marquardt algorithm was designed to approach second-order training speed without having to compute the Hessian matrix. When the performance function has the form of a sum of squares (as is typical in training feed forward networks), then the Hessian matrix can be approximated as

$$H = J^T J$$

and the gradient can be computed as

$$g = J^T e$$

Where J is the Jacobian matrix that contains first derivatives of the network errors with respect to the weights and biases, and e is a vector of network errors. The Jacobian matrix can be computed through a standard backpropagation technique that is much less complex than computing the Hessian matrix. The Levenberg-Marquardt algorithm uses this approximation to the Hessian matrix in the following Newton-like update:

$$x_{k+1} = x_k - [J^T] - \mu I]^{-1} J^T e$$

When the scalar  $\mu$  is zero, this is just Newton's method, using the approximate Hessian matrix. When  $\mu$  is large, this becomes gradient descent with a small step size. Newton's method is faster and more accurate near an error minimum, so the aim is to shift towards Newton's method as quickly as possible. Thus,  $\mu$  is decreased after each successful step (reduction in performance function) and is increased only when a tentative step would increase the performance function. In this way, the performance function will always be reduced in subsequent iterations of the algorithm.

The network utilized in this work initially takes input for first three images and predicts the next image. Subsequently the number of input image goes on increasing and the next image in the sequence is predicted. The weights are adjusted continuously according to training data.

### 5. Flame Image Recognition Experiments

The recognition experiments were carried out using a flickering flame as collected by (Sameer Dubey et al, 2010). The flame image sequence with maximum flicker was chosen to prove robustness of the method used.

#### 5.1 Flame Image Preparation

The flame image was 144x 176 pixel RGB image in BMP format. These images were captured by a CCD (charged coupled Device) in form of a video. The video sequence was decomposed into images at a frequency of 15Hz or 0.07 sec/image. A set of consecutive 50 images were

selected for analysis. Each image was individually processed to find out the location where 0.95 % intensity pixel for the flame exists. Such pixels were considered to be the edge of the image. This data was stored in a database corresponding to the image number. Fig 3 shows some of the images in the sequence with edge marked around them. The intensity of flicker may be noted in these figures. Some of the frames are arranged in sequence from left to right.

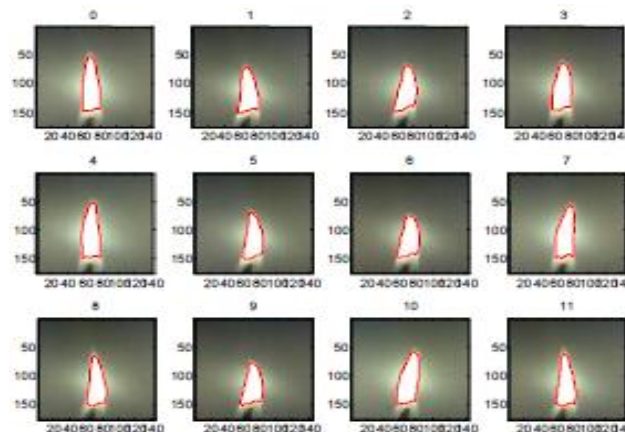


Fig 3: Images showing Intensity of Flicker in Input Images Left to right in sequence.

#### 5.2 Recognizing experiments

Back Propagation Recognition theorems were used in the prediction experiments because of their good performance. The improved back propagation algorithm Levenberg-Marquardt (L-M) algorithm was used in this experiment. After experimenting with tansig, logsig, purelin, it was found that Purelin gives the best results. Hence both transfer function for ith layer and backpropagation network training function were used to be purelin. Gradient Decent learning function was used for making the network learn. The data usage pattern for the program is shown in Fig 4. Use of very long number of training data lead to erroneous results in some cases. This was eliminated by refreshing the data set whenever mean square error went up too high. Very high refreshing rate does not give very good predictions. Hence an optimum refresh rate is maintained to get good results.

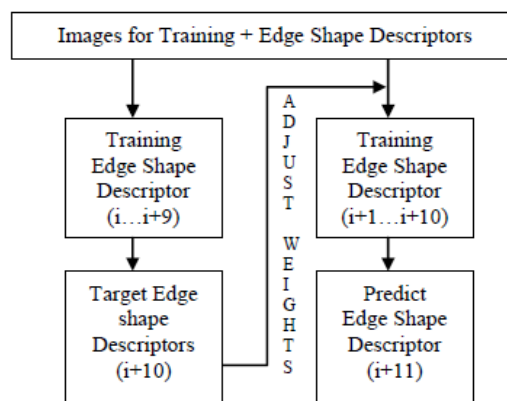
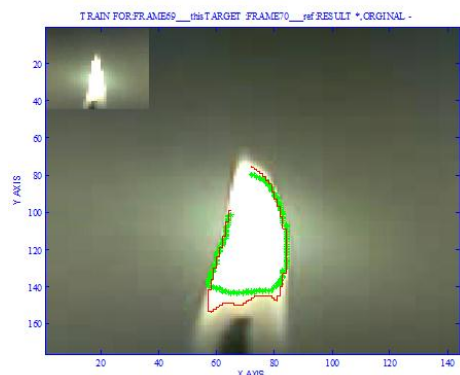
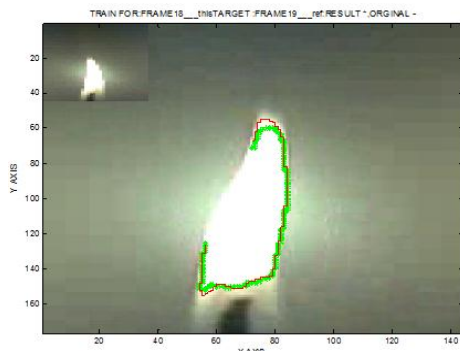


Fig 4 Flame Image data flow for Image Recognition

Fig 5 shows one of the results obtained while training the algorithm for predicting next image in sequence. Thin lines show the original boundary, while thick lines show the predicted boundary. Where the image inset shows the image to which network was trained for. An efficiency of 89% was achieved for predicting each pixel with accuracy on each image. Fig 6 shows the robustness of the algorithm in flame image prediction. The training image is left deflected but still then the algorithm computes the prediction correctly for the right deflected flame.



**Fig 5:** The flame edge predicted is shown in thick (green) lines and original edge is shown in thin lines (red). Training was given for 69th image (inset) and 70th image edge is predicted.



**Fig 6:** The flame edge predicted is shown in thick (green) lines and original edge shown in thin lines (red). Training was given for 18th image (inset) and 19th image edge is predicted.

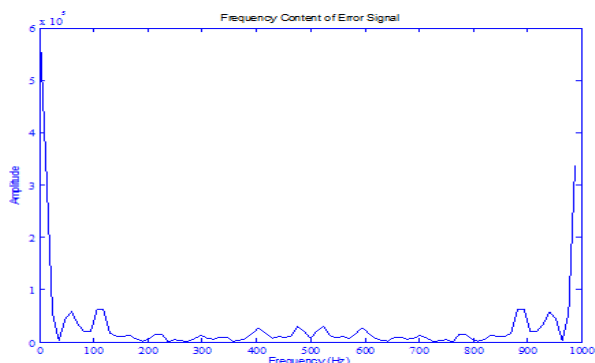


**Fig 7:** Typical frequency domain plot for the error between real and predicted flame images edges.

This algorithm was run on 50 subsequent images. Mean square error plot was obtained for prediction on each

image. It was observed that error was fluctuating between maximum and minimum value. This fluctuation is attributed to training of neural network according to change in flame shape. Hence there is a rise in mean square error in every alternate image.

When mean square error is transferred to frequency domain Fig 7 shows that frequency of 100Hz has caused high amplitude of error in flame.

$$\eta_{\text{prediction}} = 100 - \left( \frac{\sum_{\text{images}} \sum_{\text{edge pixel}} |\text{pixel error}|}{N_{\text{pixel}} * N_{\text{images}}} \right)$$

Equation (1) gives the relation used to ascertain prediction efficiency  $\eta_{\text{efficiency}}$  of the algorithm with  $N_{\text{images}}$  in the training set and  $N_{\text{pixel}}$  in flame edge of each image.  $\sum(|\text{pixel error}|)$  is sum of absolute value of error in predicting state of any edge pixel’s position.

**Conclusions**

Hence very high rate of prediction efficiency was obtained using this method. Following conclusions could be drawn out:

- 1) The coordinates of the pixels could be efficiently used as shape descriptor in image processing and prediction experiments.
- 2) An overall prediction efficiency  $\eta_{\text{prediction}}$  of 89% was obtained while predicting next image in the sequence, which was 0.07 sec away in the sequence.
- 3) For about every alternate image in the sequence the predicted edge matched with the target edge. This was because the network adjusted according to the changes in the flame shape.

Hence, this prediction algorithm is useful in all places where manual intervention is required to control a flame as per inputs of “watching flame” operation. Utility area includes rotary kiln industry, Flaring operations in petroleum refineries, fertilizer plants, and ignition lances industry.

**References**

Sameer Dubey, Aswini Bhoi, P.C.Mishra, Prabin Patnaik, Amitabh Biswas (2010), Experimental Characterization of Buoyancy Driven Enclosed Flames by using Image Processing Technique, *International Conference on Recent Advances in Mechanical Engineering*, Vol1, pp13-18

S.S. Krishnan, J. M. Abshire, P.B. Sunderland, Z.G. Yuan and J.P. Gore (2008), Analytical predictions of shapes of laminar diffusion flames in microgravity and earth gravity, *Combustion Theory and Modeling*, Vol. 12, No. 4, pp 605–620.

P.B. Sunderland, J.G. Quintiere, G.A. Tabak, D. Lian, C.-W. Chiu (2010) Analysis and measurement of candle flame shapes, *Proceedings of the Combustion Institute*, Vol No33, pp 2489-2496

Xu, F., Dai, Z. and Faeth, G.M. (2000) Flame Sheet Shapes of Nonbuoyant Laminar Coflowing Jet Diffusion Flames, *AIAA Journal*, 13, pp 253-290

Keng Hoo Chuah, Genichiro Kushida, (2000), the prediction of flame heights and flame shapes of small fire whirls, *Proceedings of the Combustion Institute*, 31, pp.2599-2606

F.C.Christo, A.R.Masri, E.M.Nabot (1996) An Integrated PDF/ Neural Network Approach For Simulating Turbulent Reacting Systems, *26th International Symposium on Combustion*, .26, pp 43-48

Zhang Hong-liang, Zou Zhong, Li Jie, Chen Xiang-Tao (2008) J. Cent. South University of Technology, *Springer publishing company*, pp.39-43.

Hamid A. Abbasi, David M Rue, C.Wagner (2004), Flex-Flame Burner and Self Optimizing Combustion system, *United States Patent*, US 6702571 B2

Mark G. Allen, Charles T Butler, Stephen A. Johnson., Edmund Y., Farla M. Russo, Integrated Imaging sensor/Neural Network Controller for Combustion systems, *United States Patent*, US5249954